Multimodality Imaging and Preclinical Evaluation of ^{177}Lu-AMBA for Human Prostate Tumours in a Murine Model

I-HSIANG LIU[1], CHIH-HSIEN CHANG[1,2], CHUNG-LI HO[1], SHU-PEI CHIU[1], WAN-CHI LEE[1], TSUI-JUNG CHANG[1], LIANG-CHENG CHEN[1], YU-HSIEN WU[1], CHENG-HUI CHUANG[1], YING-KAI FU[1] and TE-WEI LEE[1]

[1]*Institute of Nuclear Energy Research, Taoyuan, Taiwan, R.O.C.;*
[2]*Biomedical Imaging and Radiological Sciences, National Yang-Ming University, Taipei, Taiwan, R.O.C.*

Abstract. *AMBA (DO3A-CH_2CO-G-(4-aminobenzoyl)-QWAVGHLM-NH_2) is a bombesin (BN)-like peptide having high affinity with gastrin-releasing peptide receptors (GRPr). ^{177}Lu-AMBA is currently undergoing clinical trial as a systemic radiotherapy for hormone refractory prostate cancer (HRPC) patients. This study evaluated the biodistribution, pharmacokinetics, bioluminescent imaging (BLI) and microSPECT/CT imaging of ^{177}Lu-AMBA in PC-3M-luc-C6 luciferase-expressing human prostate tumour-bearing mice. Plasma stability of ^{177}Lu-AMBA could be maintained up to 55.67±6.07% at 24 h in a protection buffer. High positive correlations of PC-3M luc-C6 tumour growth in SCID mice between caliper measurement and BLI were observed (R^2=0.999). Both the biodistribution and microSPECT/CT imaging in PC-3M-luc-C6 bearing-tumour mice showed that ^{177}Lu-AMBA in tumour uptake could be retained for 24 h. The distribution half-life ($t_{1/2\alpha}$) and the elimination half-life ($t_{1/2\beta}$) of ^{177}Lu-AMBA in mice were 0.52 h and 26.6 h, respectively. These results indicated that BLI could be used to monitor the growth of tumour. High uptake of ^{177}Lu-AMBA in PC-3M-luc-C6 tumour-bearing mice by microSPECT/CT imaging can further evaluate the potential of ^{177}Lu-AMBA therapy for PC-3M-luc-C6 tumours.*

Prostate cancer is estimated to be first in the number of cancer cases and second in the number of deaths due to cancer among men in the Western world (1). The prostate-specific antigen (PSA) has been used for the diagnosis and staging of prostate cancer, and its detection sensitivity has made it effective for the evaluation of therapeutic efficacy (2). However, there are still a number of limitations that need to be addressed, such as the facts that PSA detection alone tends to underestimate the stage of prostate cancer (3) and that therapy makes prostate tumours become hormone-independent growths after treatment with androgen-deprivation therapy (4). Therefore, efforts to establish new therapeutic approaches for prostate cancer are continuing. In addition to PSA, there are other biomarkers that are overexpressed in prostate cancer such as prostate stem cell antigen (PSCA), prostate-specific membrane antigen (PSMA) (5), early prostate cancer antigen (EPCA), EPCA-2 (6) and gastrin-releasing peptide receptor (GRPr).

GRPr, one kind of G-protein-coupled receptor, is a subtype of bombesin (BN)-like peptide receptors, which are normally expressed in non-neuroendocrine tissues of the pancreas and the breast and neuroendocrine tissues of the brain, the gastrointestinal (GI) tract, the lung and the prostate, but are expressed abnormally in cancers of the prostate, the colon and the lung (7-9). Because of the hormone-independent growth of prostate cancer after androgen-deprivation therapy, overexpressed GRPrs on these tumour cells are considered a promising approach for prostate cancer therapy. BN-like peptides can target GRPr and may be considered as one kind of probe for prostate cancer (10, 11). In humans, GRPr is over-expressed in androgen-independent prostate cancer (12). The PC-3 xenograft tumour is one of the suitable models for evaluating the antineoplastic activity of BN-like peptides in the treatment of androgen-independent prostate cancer (13). AMBA (DO3A-CH_2CO-G-(4-aminobenzoyl)-QWAVGHLM-NH_2), a well-known BN-like compound, is considered to have high affinity with GRPr and NMBr (neuromedin B receptor) (14, 15). AMBA has a DO3A structure that can chelate tripositive lanthanide isotopes, such as ^{68}Ga, ^{90}Y, ^{111}In and ^{177}Lu, thus it can formulate many kinds of radiolabelled probes for various purposes (16). ^{177}Lu-AMBA is one radiolabelled probe that can be used for the diagnosis and therapy of prostate tumours. Its lack of radiostability is

Correspondence to: Dr. Chih-Hsien Chang, Isotope Application Division, Institute of Nuclear Energy Research, 1000 Wenhua Road, Chiaan Village, Lungtan, Taoyuan 325, Taiwan, R.O.C. Tel: +88 634711400 ext 7227, Fax: +88 634713491, e-mail: chchang@iner.gov.tw

Key Words: Bioluminescent imaging, bombesin (BN)-like peptides, gastrin-releasing peptide receptors, prostate cancer.

its only disadvantage but this can be addressed by mixing it with a protection buffer of ascorbic acid (17). In a previous study, not only did the PC-3 cell line express high GRPr, but also the LNCaP and DU145 cell line expressing low GRPr could be effectively treated by ^{177}Lu-AMBA (18). Overall, ^{177}Lu-AMBA is a promising drug for prostate cancer and is already in phase I clinical trials (14).

Bioluminescent imaging (BLI) is often applied for tumour model systems and it can be used to monitor tumour growth (19). PC-3M-luc-C6 is a PC-3 cell expressing firefly luciferase, which has been proven to be an efficient and sensitive measure for prostate cancer in murine models (20). In this study, the growth of PC-3M-luc-C6 tumour in SCID mice was evaluated using a BLI system. Although previous studies have demonstrated the radiostability, binding properties *in vitro* and biodistribution *in vivo* (14), the pharmacokinetics and microSPECT/CT imaging of ^{177}Lu-AMBA in PC-3M-luc-C6 xenograft SCID mice have not yet been reported. In-depth *in vivo* studies of ^{177}Lu-AMBA could help to evaluate its properties. Furthermore, combining BLI and microSPECT/CT imaging could have the potential for evaluating the therapeutic efficacy of ^{177}Lu-AMBA at early disease stages.

Materials and Methods

Chemicals. Protected N$^{\alpha}$-Fmoc-amino acid derivatives were obtained from Novabiochem (Merck Schuchardt OHG, Germany), Fmoc-amide resin and coupling reagent were obtained from Applied Biosystems Inc. (Foster City, CA, USA) and DOTA-tris (*t*-Bu ester) was obtained from Macrocyclics (Dallas, TX, USA). Fmoc-4-abz-OH was obtained from Bachem (Chauptstrasse, Switzerland). Bombesin was obtained from Fluka (Buchs, Switzerland).

Synthesis of AMBA. AMBA was synthesized using solid-phase peptide synthesis (SPPS) using an Applied Biosystems Model 433A equipped with an automated peptide synthesizer, employing the Fmoc (9-fluorenylmethoxy-carbonyl) strategy. Carboxyl groups on Fmoc-protected amino acids were activated by (2-(1-*H*-benzotriazol-1-yl)-1,1,3,3-tetramethyluronium hexafluorophosphate (HBTU), forming a peptide bond with the *N*-terminal amino group on the growing peptide, anchored *via* the *C*-terminus to the resin, and providing for stepwise amino acid addition. Rink Amide resin (0.25 mM) and Fmoc-protected amino acids (1.0 mM), with appropriate side chain protections, and DOTA-tris (*t*-Bu ester) were used for SPPS of the BBN conjugates. Side chain protecting groups in the synthesis were Trt for Gln and His, and Boc for Trp.

The protected peptide-resin was cleaved and deprotected with a mixture of 50% trifluoroacetic acid (TFA): 45% chloroform, 3.75% anisole, 1.25% 1, 2-ethanedithiol (EDT) for 4 h at room temperature (RT). The crude peptide was isolated by precipitating with cool diethyl ether. After centrifugation, the collected precipitate was dried under vacuum. The crude peptide sample was purified by reverse phase high-performance liquid chromatography (HPLC) using a column of XTerra prep, MSC18, 5 μm, 18×50 mm (Waters Corp., MA, USA) with an acetonitrile/water gradient consisting of solvent A (0.1% TFA in H_2O) and solvent B (0.1% TFA in acetonitrile), with a 14.8% yield; flow: 6 ml/min; gradient: 80% A–40% B for 20 min. The molecular weight was determined with a MALDI-TOF mass spectrometer (Bruker Daltonics Inc, Germany). M/z determined for the peptide was: AMBA, 1,502.6 [M+H].

Radiolabelling and purification of ^{177}Lu-AMBA. The labelling method for AMBA with ^{177}Lu was previously described (14). Briefly, 3 μg of AMBA and about 37 MBq 177LuCl (PerkinElmer, USA; 37 GBq/ml in 0.05 M HCl) were added in 0.2 M sodium acetate (pH4.8) until there was 50 μl per vial, and then heated at 95˚C for 10 min. The labelling efficiency of ^{177}Lu-AMBA was analysed by instant thin-layer chromatography (ITLC SG; Pall Corporation, New York, NY, USA) with 0.1 M Na-citrate (pH 5.0) as solvent ($^{177}LuCl_3$: Rf=0.9~1.0, peptide-bound ^{177}Lu: Rf=0~0.1) (17). Radiocolloid was also monitored using ITLC strips developed with acetone/0.9% saline (1:1) as solvent (radiocolloid: Rf=0~0.1). Radio high performance liquid chromatography (Radio-HPLC) analysis was performed using a Waters 2690 chromatography system with a 996 photodiode array detector (PDA), a Bioscan radiodetector (Washington, DC, USA) and a FC 203B fraction collector by Gilson (Middleton, WI, USA). 177Lu-AMBA was purified by an Agilent (Santa Clara, CA, USA) Zorbax bonus-RP HPLC column (4.6×250 mm, 5 μm) eluted with a gradient mixture from 80% solvent A (0.1% TFA in H_2O) (v/v)/20% B (0.1% TFA in acetonitrile) (v/v) to 70% A/30% B in 15 min. Flow rate was 1.5 ml/min at RT and the retention time for ^{177}Lu-AMBA was 7.5 min.

In vitro plasma stability. After radiolabelling, ^{177}Lu-AMBA (10 μl, 7.4 MBq) was first diluted with 40 μl protection buffer [8:2 mixture of 0.9% sodium chloride injection USP and ascorbic acid (250 mg/ml; Tai Yu Chemical & Pharmaceutical, Taiwan, ROC), with 0.025% (w/v) Na_2EDTA], and the same volume of 0.9% sodium chloride injection USP was used as a control. The sample was incubated in normal saline, rat and human plasma at a ratio of 1:1 (v/v) at 37˚C. At several time points after administration (1, 4, 8, 24 and 48 h), 1 μl and 5μl of ^{177}Lu-AMBA in plasma or normal saline were analyzed using ITLC-SG and radio-HPLC, respectively. The analysis method was the same as that applied for purification.

Cell culture and animal model. Bioluminescent human prostate adenocarcinoma cell line PC-3M-luc-C6 (Caliper Life Sciences, MA, USA) was maintained in Ham's F-12K medium supplemented with 10% heat-inactivated fetal bovine serum and incubated in 5% CO_2 at 37˚C, and subcultured by 0.05% trypsin/ethylenediamineteraacetic acid (all from GIBCO, Grand Island, NY, USA). The cell line was thawed from an aliquot vial, grown and used within 10 passages for animal inoculation. Male severely compromised immunodeficient (SCID) mice at 4 weeks old were obtained from the Laboratory Animal Center of National Taiwan University (Taipei, Taiwan, ROC) and maintained on a standard diet (Lab diet; PMI Feeds, St. Louis, MO, USA) at RT, with free access to tap water in the animal house of the Institute of Nuclear Energy Research (INER), Taoyuan, Taiwan, ROC. Each of the SCID mice was subcutaneously injected with 2×10^6 PC-3M-luc-C6 cells (in 100 μl of 0.9% sodium chloride injection USP) in the right-hind flank. The animal experiments were approved by the Institutional Animal Care and Use Committee (IACUC) of the INER.

BLI. BLI was performed with a highly sensitive, cooled CCD camera mounted in a light-tight specimen box (IVIS Imaging System 100 Series; Xenogen, USA) using protocols similar to those

Table I. *In vitro stability of ^{177}Lu-AMBA by HPLC analysis at different time points after incubation in normal saline, human plasma and rat plasma at 37˚C (mean±SEM, n=4 at each time point).*

Time point (h)	Control			With protection buffer		
	Normal saline (%)	Rat plasma (%)	Human plasma (%)	Normal saline (%)	Rat plasma (%)	Human plasma (%)
0	70.8±7.51	74.3±7.58	75.7±8.86	71.4±12.5	71.4±12.5	71.4±12.5
1	63.6±11.5	65.1±12.0	78.4±5.97	67.3±6.94	73.4±8.47	73.2±11.0
4	52.9±12.2	58.7±19.7	69.9±3.60	66.7±10.0	68.7±1.57	68.7±10.8
24	14.8±13.0	25.0±18.1	57.5±10.1	55.7±6.07	26.7±2.18	47.1±5.64
48	0.00±0.00	24.3±21.9	46.8±13.0	38.4±3.83	15.1±4.63	29.7±0.68

described previously (21). For *in vitro* imaging, bioluminescent cells were diluted from 10,000 to 20 cells into appropriate cell culture media in black, clear bottom, 96-well plates. The luciferase activity was measured by adding 200 μl luciferase reagents (150 μg/ml) (Xenogen, Alameda, CA, USA) 10 min prior to imaging. Quantification of signals in the regions of interest (ROI) from displayed images were designated around each well by grid mode and quantified as total photon counts or photons/s using the Living Image software (Xenogen). Background bioluminescence from the imaging box was in the range of 1×10^4 photons or $1\text{-}2\times10^5$ photons/s.

For *in vivo* BLI, five PC-3M-luc-C6 tumour-bearing mice were given the substrate D-luciferin in DPBS intraperitoneally at 150 mg/kg. 10-15 min after luciferin injection, five mice were placed onto the stage inside the light-tight camera box with continuous exposure of 1-2% isoflurane and imaged with the IVIS system. Imaging time ranged from 30 s to 2 min, depending upon tumour bioluminescence and size. ROIs from displayed images were designated around the tumour sites and quantified as total photons/s by the Living Image software.

Biodistribution. At 3 weeks after PC-3M-luc-C6 cell inoculation, developed tumour weights ranged from 0.01 to 0.2 g. Twenty-four PC-3M-luc-C6 xenograft SCID mice (n=4 for each group) were injected with 0.37 MBq (0.1 μg) of the 177Lu-AMBA in 80 μl of 0.9% sodium chloride injection USP *via* the tail vein. The mice were sacrificed by CO_2 asphyxiation and tissues and organs were excised at 30 min, 1, 4, 8, 24 and 48 h post injection (*p.i.*). Subsequently, the tissues and organs were weighed, radioactivity was counted in a Packard Cobra II gamma-counter by Perkin-Elmer (Waltham, MA, USA) and the percentage of injected dose per gram (% ID/g) for each organ or tissue were calculated (22).

Pharmacokinetic studies. Four PC-3M-luc-C6 xenograft SCID mice were injected with 0.37 MBq (0.1 μg) of the ^{177}Lu-AMBA in 80 μl of 0.9% sodium chloride injection USP *via* the tail vein. At 5 min, 1, 4, and 24h *p.i.*, 20 μl of blood was collected from the heart puncture, then the blood weighed and radioactivity was counted in the Cobra II gamma-counter and the percentage of injected dose per gram (% ID/g) was calculated. The data were fitted to a two-compartment model and the pharmacokinetic parameters were derived by the WinNonlin 5.0 software (Pharsight Corporation, Mountain View, CA, USA).

Micro-SPECT/CT imaging. Two male SCID mice bearing human PC-3M-luc-C6 tumours of approximately 0.1 g were *i.v.* injected with 14.8 MBq/0.95 μg ^{177}Lu-AMBA after purification by radio-HPLC. The SPECT and CT images were acquired by a micro-SPECT/CT scanner system (XSPECT; Gamma Medica-ideas Inc., Northridge, CA, USA). SPECT imaging was performed using medium-energy, parallel-hole collimators at 1, 4, 8, 24, and 48 h. The source and detector were mounted on a circular gantry allowing them to rotate 360 degrees around the subject (mouse) positioned on a stationary bed. The field of view (FOV) was 12.5 cm. The imaging acquisition was accomplished using 64 projections at 90 seconds per projection. The energy windows were set at 113 keV±10% and 209 keV±10%. SPECT imaging was followed by CT imaging (X-ray source: 50 kV, 0.4 mA; 256 projections) with the animal in exactly the same position. A three dimensional (3-D) Feldkamp cone beam algorithm was used for CT image reconstruction and a two-dimensional (2-D) filtered back projection algorithm was used for SPECT image reconstruction. All image processing software, including SPECT/CT co-registration, were provided by Gamma Medica-Ideas Inc (Northridge, CA, USA). After co-registration, both the fused SPECT and CT images had 256×256×256 voxels with an isotropic 0.3-mm voxel size.

Results

Radiolabelling and plasma stability studies of ^{177}Lu-AMBA. The labelling efficiency of ^{177}Lu-AMBA by ITLC analysis was 91.14±2.59%. The protection buffer may have affected the stability of ^{177}Lu-AMBA in different conditions by radio-HPLC analysis (Table I). For radiolabelling of ^{177}Lu-AMBA, the radiochemical purity was 70.8±7.51% by radio-HPLC analysis. The stability of ^{177}Lu-AMBA rapidly reduced at 24 h and completely degraded at 48 h in normal saline without the protection buffer. However, ^{177}Lu-AMBA retained 55.67±6.07% and 38.44±3.83% at 24 and 48 h in the protection buffer, respectively. These results indicated the effect of the protection buffer on the storage of ^{177}Lu-AMBA. The stability of ^{177}Lu-AMBA in rat and human plasma without the protection buffer was not significantly different from that with the protection buffer. The stability of ^{177}Lu-AMBA in human plasma was slightly higher than that in rat plasma.

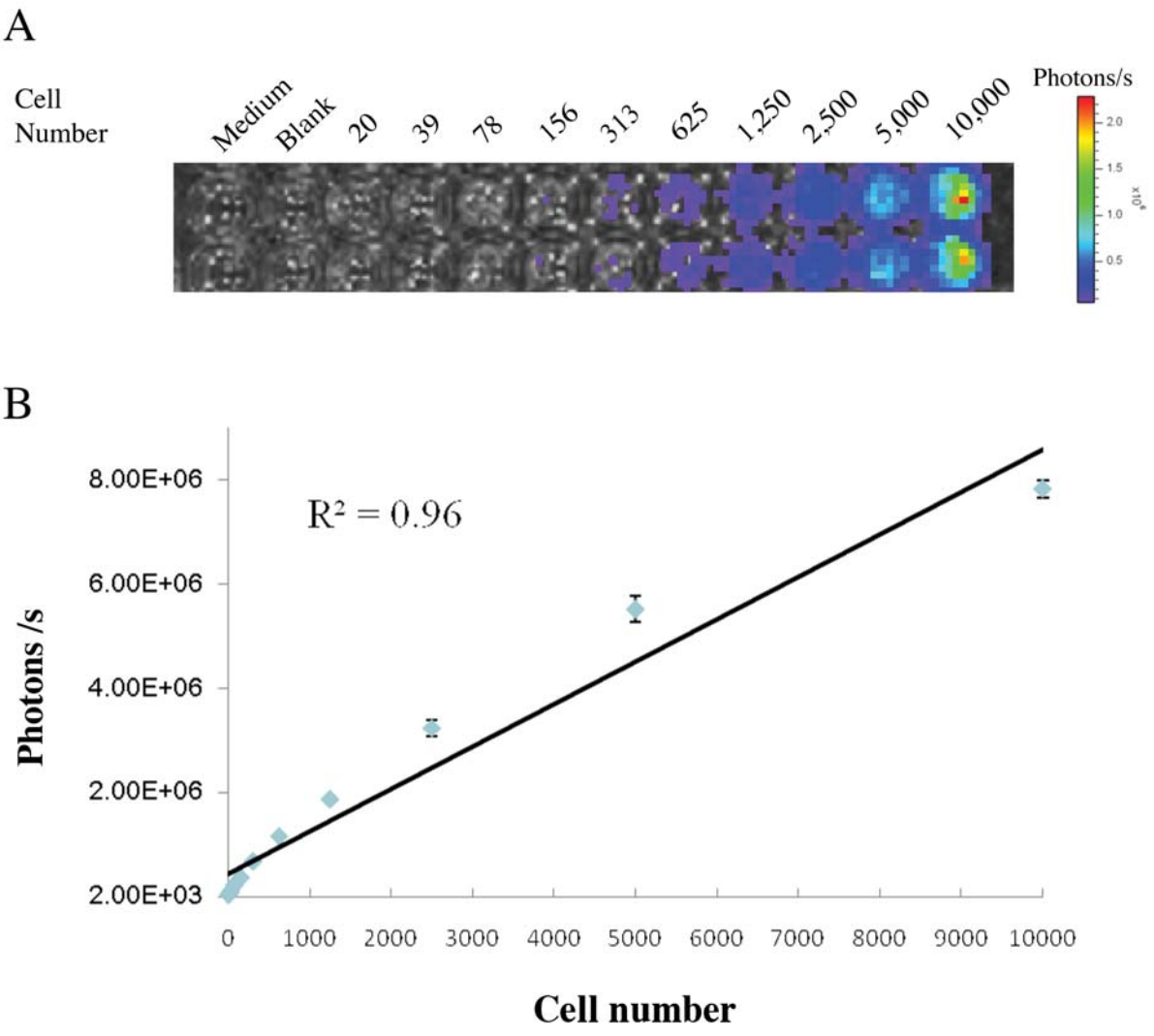

Figure 1. *Bioluminescence of human PC-3M-luc-C6 tumour cell lines expressing luciferase in vitro. (A) PC-3M-luc-C6 was diluted from 10,000 to 20 cells, plated in duplicate wells and imaged after the addition of luciferin to the media. Wells containing cells (no luciferin; column "Blank") or media only (column "Medium") served as negative controls. (B) Correlation between mean cell number per well and mean bioluminescence (photons/s per well); r^2=0.96.*

BLI. The photon emission from suspensions of human prostate (PC-3M-luc-C6) tumour cell lines expressing luciferase is shown in Figure 1A. The minimum number of detectable cells in the suspension was approximately 156 cells per well. Bioluminescence per well correlated to the total number of PC-3M-luc-C6 cells (r^2=0.96; Figure 1B). To evaluate the tumour growth *in vivo*, the subcutaneous growth of the PC-3M-luc-C6 tumour cells was sequentially measured from day 0 to day 14 by BLI and compared to external caliper measurements of the same tumour sites. On day 0, xenografted mice showed successful tumour imaging by BLI (Figure 2A). Bioluminescent photon counts in the tumour sites correlated to the growth of PC-3M-luc-C6 cells during the study period (r^2=0.96; Figure 2B). In contrast, accurate measurements of tumour volume by the caliper method could be obtained in mice only after 7 days post implantation (Figure 3A). After tumours were measurable by the caliper method, BLI correlated well with caliper-measured data (r^2=0.99; Figure 3B).

Biodistribution. ^{177}Lu-AMBA significantly accumulated in the tumour, the adrenal, the pancreas, the small intestine and large intestines (Table II). Fast blood clearance and fast excretion from the kidneys were observed. This indicated that the radioactivity was excreted rapidly in the urine. The uptake of ^{177}Lu-AMBA still remained 10.4±3.49, 3.52±0.17

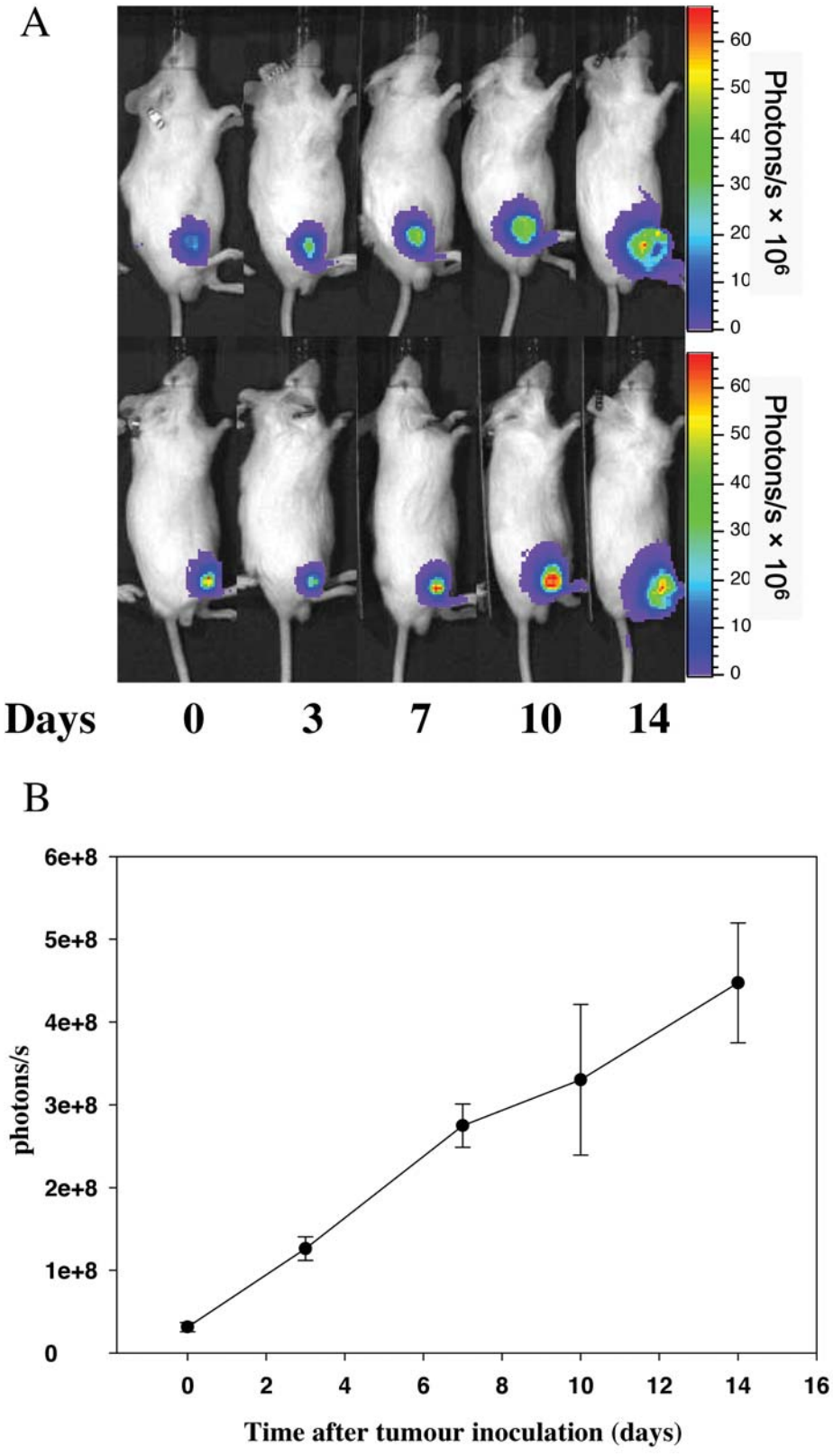

Figure 2. *Growth of PC-3M-luc-C6 tumours in SCID mice. A: Bioluminescent images of two SCID mice are displayed on day 0, 3, 7, 10 and 14. B: Tumour size was measured by calipers (n=5, mean±SEM).*

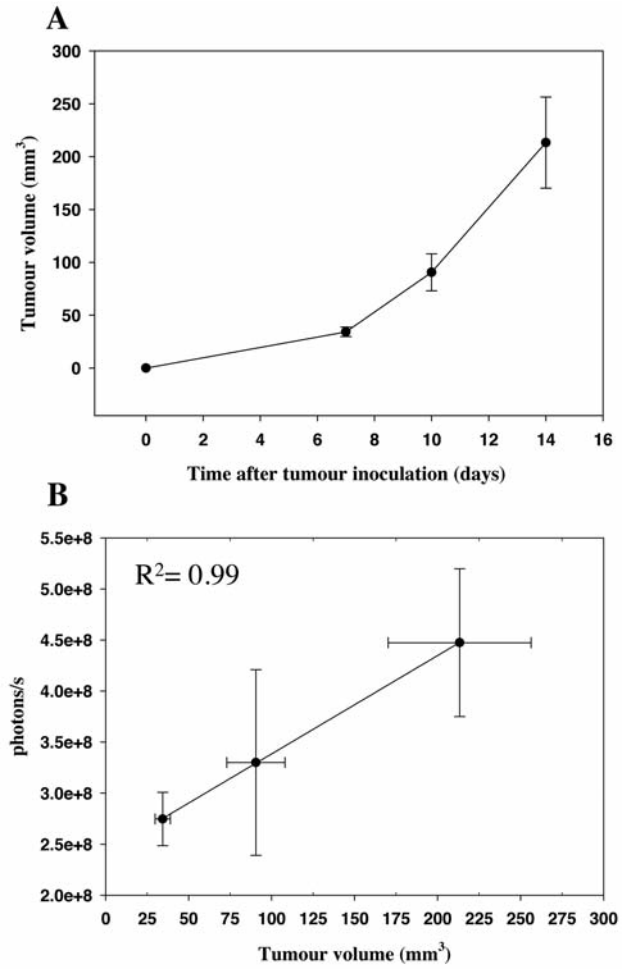

Figure 3. *Effect of bioluminescence in measuring tumour size. A: Tumour size was measured by bioluminescence (n=5, mean±SEM). B: Correlation of tumour size measured by bioluminescence and by calipers (n=5, mean±SEM).*

and 1.32±0.61% ID/g in the pancreas, the kidney and the tumour at 24 h, respectively (Table II). The tumour-to-blood ratio reached a maximum within 24 h and then declined.

Pharmacokinetic studies. The mean radioactivity (% ID/ml) of ^{177}Lu-AMBA with log scale in the plasma is plotted in Figure 4. The radioactivity declined to under detection limit after 24 h. The pharmacokinetic parameters derived by a two-compartment model (23) indicated that the distribution half-life ($t_{1/2\alpha}$) and elimination half-life ($t_{1/2\beta}$) of ^{177}Lu-AMBA were 0.52±0.05 h and 26.63±11.74 h, respectively (Table III).

MicroSPECT/CT imaging. Micro-SPECT/CT imaging of ^{177}Lu-AMBA demonstrated a significant uptake in the tumours at 4 and 24 h after intravenous injection (Figure 5). The longitudinal micro-SPECT/CT imaging showed high accumulation of ^{177}Lu-AMBA in the kidney, the pancreas

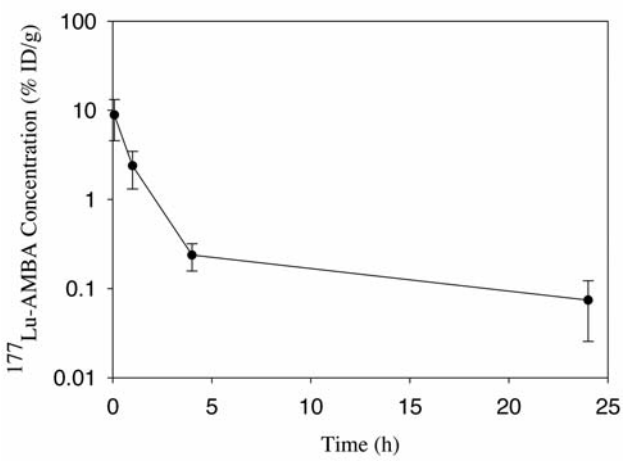

Figure 4. *Pharmacokinetics of ^{177}Lu-AMBA in PC-3M-luc-C6 tumour xenograft SCID mice after intravenous injection. Data are presented for 5 min, 1, 4, and 24 h (n=3, mean±SEM).*

and the GI tract at 4, 8, 24 and 48 h after intravenous injection. The trend of the uptake shown in the imaging data was similar to the results of the biodistribution study.

Discussion

GRP receptors are expressed in many kinds of cancers, and bombesin shows a high affinity for the GRP receptor, which has led to the development of the most appropriate radiolabelled analogues of the BN-like peptide (24, 25). ^{177}Lu-AMBA was developed (14) due to its high-affinity binding of GRP-R expressing cells (15, 17, 18, 26). Although excellent probes have been evaluated in treating prostate cancer, no study on the plasma stability of ^{177}Lu-AMBA in the protection buffer up to 72 h has yet been reported. Furthermore, multi-imaging modalities to monitor the growth of PC-3M-luc-C6 tumour by a bioluminescence system and to measure the uptake of ^{177}Lu-AMBA by microSPECT/CT have also not yet been reported.

For the plasma stability of ^{177}Lu-AMBA, the results of ITLC analysis could not distinguish the stability of 177Lu-AMBA in different environments (data not shown), whereas HPLC analysis was able to determine the decrease in the stability of ^{177}Lu-AMBA during the study period (Table I). Taken together, these data indicated that ITLC analysis is suitable only for labeling yields but not for radiochemical purity. The stability of ^{177}Lu-AMBA in normal saline decreased rapidly when no protection buffer was added and was completely degraded in 48 h, whereas 38.4±3.83% of ^{177}Lu-AMBA was contained in the protection buffer after 48 h (Table I). These results were in agreement with a previous report by Chen *et al*. (17). Although there were no significant differences whether mixing with the protection buffer in the

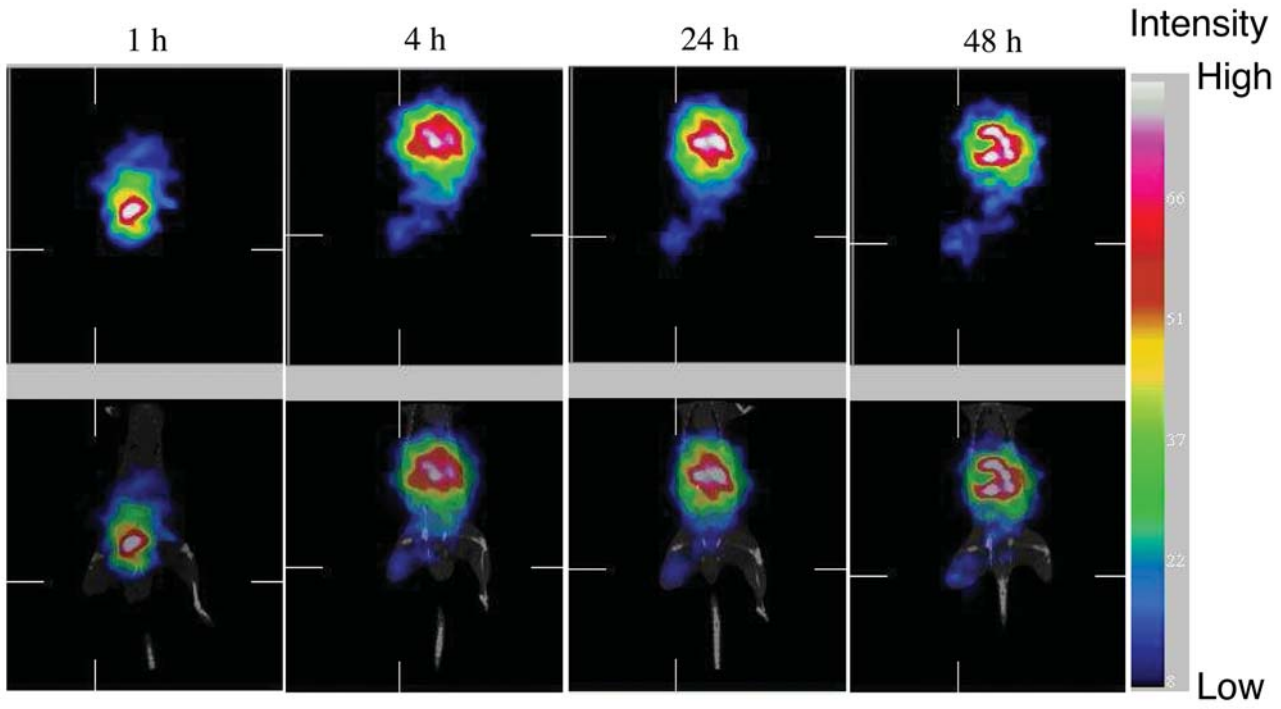

Figure 5. *Micro-SPECT/CT imaging of ^{177}Lu-AMBA was performed in PC-3M-luc-C6 tumour-bearing mice. Mice were intravenously injected with 14.8 MBq/0.95 μg ^{177}Lu-AMBA. The energy windows and the image size were set at 113 keV±10%, 209 keV±10% and 80×80 pixels, respectively.*

Table II. *Biodistribution of ^{177}Lu-AMBA after i.v. injection in PC-3M-luc-C6 prostate tumour-bearing SCID mice. Values are expressed as % ID/g, mean±SEM (n=4 at each time point).*

Organ/time	0.5 h	1 h	4 h	8 h	24 h	48 h
Blood	2.01±0.46	0.69±0.09	0.04±0.00	0.02±0.01	0.01±0.00	0.00±0.00
Brain	0.07±0.01	0.03±0.01	0.02±0.00	0.01±0.00	0.00±0.00	0.00±0.00
Muscle	0.53±0.15	0.32±0.05	0.02±0.02	0.04±0.01	0.03±0.01	0.01±0.01
Bone	0.52±0.07	0.35±0.02	0.27±0.05	0.18±0.02	0.20±0.04	0.16±0.04
Spleen	0.96±0.16	0.61±0.06	0.47±0.11	0.77±0.38	0.36±0.07	0.22±0.10
Pancreas	18.5±4.10	19.0±1.33	25.6±16.9	15.9±2.57	10.5±3.49	7.81±1.05
S.I.	1.47±0.27	1.55±0.42	1.88±1.10	0.67±0.10	0.41±0.06	0.37±0.13
L.I.	2.29±0.45	1.62±0.28	3.79±2.19	1.72±0.25	1.18±0.10	0.39±0.07
Stomach	1.81±0.38	1.20±0.21	1.24±0.46	0.58±0.10	0.39±0.03	0.34±0.02
Kidney	8.07±0.94	6.05±0.94	4.70±0.91	5.22±0.51	3.52±0.17	2.17±0.09
Bladder	5.06±1.40	2.95±1.43	0.40±0.26	0.30±0.08	0.15±0.04	0.13±0.02
Testis	0.49±0.09	0.37±0.16	0.08±0.03	0.05±0.01	0.05±0.02	0.02±0.01
Liver	0.91±0.15	0.58±0.13	0.49±0.13	0.24±0.03	0.25±0.02	0.21±0.02
Heart	0.65±0.13	0.25±0.04	0.10±0.04	0.07±0.02	0.02±0.01	0.02±0.01
Lung	1.62±0.34	0.43±0.15	0.21±0.07	0.15±0.03	0.11±0.05	0.07±0.02
Tumour	2.33±0.52	1.07±0.11	0.88±0.48	0.73±0.04	0.45±0.09	0.33±0.03
Faeces	0.77±0.12	1.12±0.43	7.22±5.52	0.80±0.21	1.29±0.34	1.09±0.15
Urine	518.8±69.29	644.1±45.64	16.0±10.23	1.17±0.37	1.36±0.42	1.61±0.28

S.I.: Small intestine; L.I.: Large intestine.

Table III. *Pharmacokinetic parameters of plasma in PC-3M-luc-C6 tumour-bearing mice after intravenous injection of ^{177}Lu-AMBA (10 μg/mouse).*

Parameter	Unit	Value
A	% ID/g	12.2±2.02
B	% ID/g	0.15±0.10
α	1/h	1.35±0.14
β	1/h	0.04±0.02
$AUC_{0\text{-}168h}$	h×(% ID/g)	12.6±1.16
$t_{1/2\alpha}$	h	0.52±0.05
$t_{1/2\beta}$	h	26.6±11.7
C_{max}	% ID/g	12.3±1.92

A, B, α, β: macro rate constants; $t_{1/2\alpha}$, $t_{1/2\beta}$: distribution and elimination half-lifes; $AUC_{0\text{-}168h}$: area under concentration of ^{177}Lu-AMBA *versus* time curve; C_{max}: maximum concentration in plasma.

rat or human plasma, the reduction of ^{177}Lu-AMBA in the rat plasma was faster than in the human plasma. The decrease of ^{177}Lu-AMBA in plasma may be due to cleavage by metalloproteases (27) and the different amounts and kinds of metalloproteases in rat and human plasma.

To evaluate the bioluminescent PC-3M-luc-C6 tumour model for the ^{177}Lu-AMBA therapeutic study, the cell number had a good positive correlation with the photon emission from the *in vitro* study (Figure 1). The results showed a distinct advantage of BLI over traditional approaches for monitoring the growth of tumours in mice (Figure 2). The high sensitivity of BLI was effectively demonstrated in the subcutaneous models where tumours were not measurable by caliper but could be quantified by photon emissions. This early detection of tumour growth permitted the drug study using PC-3M-luc-C6 to be initiated in mice with barely palpable tumours and to be completed with end-point tumours smaller than those in standard models using caliper measurements (19). Since BLI reflects the number of metabolically active tumour cells rather than a volumetric measurement of tumour mass, it may offer a closer assessment of treatment efficacy on tumour physiology than other detection methods. Non-invasive and sequential molecular imaging can serve as an accurate guide in diagnostic and therapeutic studies since the tumour growth and therapeutic response in each animal can be immediately assessed rather than rely on data from sacrificed animals at designated time points (28). As a result, non-invasive molecular imaging requires fewer experimental animals than conventional invasive detection methods. Optical imaging techniques represent a low cost and quick modality for real-time analysis of gene expression in small animal models though they are limited by depth penetration and cannot be applied to humans easily (29).

The biodistribution of ^{177}Lu-AMBA in PC-3M-luc-C6 bearing mice was similar to that of the PC-3 tumour model (14). ^{177}Lu-AMBA was excreted primarily by the urine and accumulated most in the pancreas, in addition to the kidneys, the GI tract and the tumour (Table II). Compared to other BN-analogues, the rapid excretion of urine makes ^{177}Lu-AMBA suitable for radiotherapy since there is less detrimental effect to other organs from the radiation. Although GRPr is a predominant receptor subtype in the pancreas of rodents, such high uptake of ^{177}Lu-AMBA in the tumour may not affect the physiological condition in mice (22). Roger *et al*. found that the concentration of GRPrs on the mouse pancreas was 27 fmol/mg (30), while Fanger *et al*. reported a level of 75 fmol/mg (31). The higher pancreas uptake of the radiolabelled bombesin agonist may be due to its higher metabolic stability *in vivo*. Waser *et al*. reported that, in contrast to the strongly labelled GRPR-positive mouse pancreas with ^{177}Lu-AMBA, the human pancreas did not bind ^{177}Lu-AMBA unless chronic pancreatitis was diagnosed (15). In the pharmacokinetic studies (Figure 4 and Table III), the elimination half-life ($t_{1/2\beta}$), distribution half-life ($t_{1/2\alpha}$) and the area under the concentration curve (AUC) of ^{177}Lu-AMBA demonstrated the behaviour of fast peptide distribution and elimination.

In contrast to BLI, radionuclide-based techniques have good spatial resolution though they are somewhat limited by their higher cost and production of isotopes. Various methodologies have been developed for imaging the reporter gene expression in living cells, non-invasively and repetitively in animals. Each of these modalities has unique applications, advantages and limitations that can be complementary to other modalities (32). Micro-SPECT/CT imaging is a non-invasive imaging modality that can determine the distribution of radiotherapeutic drugs *in vivo* at different time points. Micro-SPECT/CT imaging correlated well with the biodistribution study. ^{177}Lu-AMBA was clearly distributed in the pancreas, the GI tract and the tumour 4 to 48 h after administration (Figure 5). Many studies have focused on micro-SPECT/CT imaging of BN-analog and AMBA, which were labeled with ^{111}In (21, 33-35). Recently, imaging of ^{177}Lu-AMBA by Maddalena *et al*. using planar gamma imaging showed results similar to the present study (18). Overall, micro-SPECT/CT imaging can be a very accurate tool for evaluating the quantity and quality of radiotherapy. In conclusion, the BLI system could effectively evaluate the PC-3M-luc-C6 tumour model and, combined with experiments of ^{177}Lu-AMBA *in vitro* and *in vivo*, provides a multimodality imaging method for the preclinical study of ^{177}Lu-AMBA.

Acknowledgements

The Authors would like to thank Chun-Lin Chen for his help with the preparation of AMBA.

References

1 Jemal A, Siegel R, Ward E, Hao Y, Xu J and Thun MJ: Cancer statistics, 2009. CA Cancer J Clin *59*: 225-249, 2009.

2 Stamey TA, Yang N, Hay AR, McNeal JE, Freiha FS and Redwine E: Prostate-specific antigen as a serum marker for adenocarcinoma of the prostate. N Engl J Med *317*: 909-916, 1987.

3 D'Amico AV, Whittington R, Schnall M, Malkowicz SB, Tomaszewski JE, Schultz D and Wein A: The impact of the inclusion of endorectal coil magnetic resonance imaging in a multivariate analysis to predict clinically unsuspected extraprostatic cancer. Cancer *75*: 2368-2372, 1995.

4 Raghavan D and Rogers J: Update in the management of prostate cancer. Med J Aust *152*: 419-426, 1990.

5 Ananias HJ, van den Heuvel MC, Helfrich W and de Jong IJ: Expression of the gastrin-releasing peptide receptor, the prostate stem cell antigen and the prostate-specific membrane antigen in lymph node and bone metastases of prostate cancer. Prostate *69*: 1101-1108, 2009.

6 Hansel DE, DeMarzo AM, Platz EA, Jadallah S, Hicks J, Epstein JI, Partin AW and Netto GJ: Early prostate cancer antigen expression in predicting presence of prostate cancer in men with histologically negative biopsies. J Urol *177*: 1736-1740, 2007.

7 Sunday ME: Tissue-specific expression of the mammalian bombesin gene. Ann N Y Acad Sci *547*: 95-113, 1988.

8 Woodruff GN, Hall MD, Reynolds T and Pinnock RD: Bombesin receptors in the brain. Ann NY Acad Sci *780*: 223-243, 1996.

9 Nagy A and Schally AV: Targeting cytotoxic conjugates of somatostatin, luteinizing hormone-releasing hormone and bombesin to cancers expressing their receptors: a 'smarter' chemotherapy. Curr Pharm Des *11*: 1167-1180, 2005.

10 Schroeder RP, van Weerden WM, Bangma C, Krenning EP and de Jong M: Peptide receptor imaging of prostate cancer with radiolabelled bombesin analogues. Methods *48*: 200-204, 2009.

11 Aprikian AG, Han K, Guy L, Landry F, Begin LR and Chevalier S: Neuroendocrine differentiation and the bombesin/gastrin-releasing peptide family of neuropeptides in the progression of human prostate cancer. Prostate Suppl *8*: 52-61, 1998.

12 Markwalder R and Reubi JC: Gastrin-releasing peptide receptors in the human prostate: relation to neoplastic transformation. Cancer Res *59*: 1152-1159, 1999.

13 Reile H, Armatis PE and Schally AV: Characterization of high-affinity receptors for bombesin/gastrin releasing peptide on the human prostate cancer cell lines PC-3 and DU-145: internalization of receptor bound ^{125}I-(Tyr^4) bombesin by tumor cells. Prostate *25*: 29-38, 1994.

14 Lantry LE, Cappelletti E, Maddalena ME, Fox JS, Feng W, Chen J, Thomas R, Eaton SM, Bogdan NJ, Arunachalam T, Reubi JC, Raju N, Metcalfe EC, Lattuada L, Linder KE, Swenson RE, Tweedle MF and Nunn AD: ^{177}Lu-AMBA: Synthesis and characterization of a selective ^{177}Lu-labeled GRP-R agonist for systemic radiotherapy of prostate cancer. J Nucl Med *47*: 1144-1152, 2006.

15 Waser B, Eltschinger V, Linder K, Nunn A and Reubi JC: Selective *in vitro* targeting of GRP and NMB receptors in human tumours with the new bombesin tracer ^{177}Lu-AMBA. Eur J Nucl Med Mol Imaging *34*: 95-100, 2007.

16 Tweedle MF: Peptide-targeted diagnostics and radiotherapeutics. Acc Chem Res *42*: 958-968, 2009.

17 Chen J, Linder KE, Cagnolini A, Metcalfe E, Raju N, Tweedle MF and Swenson RE: Synthesis, stabilization and formulation of ^{177}Lu-AMBA, a systemic radiotherapeutic agent for Gastrin Releasing Peptide receptor positive tumors. Appl Radiat Isot *66*: 497-505, 2008.

18 Maddalena ME, Fox J, Chen J, Feng W, Cagnolini A, Linder KE, Tweedle MF, Nunn AD and Lantry LE: ^{177}Lu-AMBA biodistribution, radiotherapeutic efficacy, imaging, and autoradiography in prostate cancer models with low GRP-R expression. J Nucl Med *50*: 2017-2024, 2009.

19 Jenkins DE, Oei Y, Hornig YS, Yu SF, Dusich J, Purchio T and Contag PR: Bioluminescent imaging (BLI) to improve and refine traditional murine models of tumor growth and metastasis. Clin Exp Metastasis *20*: 733-744, 2003.

20 Jenkins DE, Yu SF, Hornig YS, Purchio T and Contag PR: *In vivo* monitoring of tumor relapse and metastasis using bioluminescent PC-3M-luc-C6 cells in murine models of human prostate cancer. Clin Exp Metastasis *20*: 745-756, 2003.

21 Ho CL, Chen LC, Lee WC, Chiu SP, Hsu WC, Wu YH, Yeh CH, Stabin MG, Jan ML, Lin WJ, Lee TW and Chang CH: Receptor-binding, biodistribution, dosimetry, and micro-SPECT/CT imaging of ^{111}In-[DTPA^1, Lys^3, Tyr^4]-bombesin analog in human prostate tumor-bearing mice. Cancer Biother Radiopharm *24*: 435-443, 2009.

22 Smith CJ, Gali H, Sieckman GL, Hayes DL, Owen NK, Mazuru DG, Volkert WA and Hoffman TJ: Radiochemical investigations of ^{177}Lu-DOTA-8-Aoc-BBN[7-14]NH2: an *in vitro/in vivo* assessment of the targeting ability of this new radiopharmaceutical for PC-3 human prostate cancer cells. Nucl Med Biol *30*: 101-109, 2003.

23 Chang CH, Chou TK, Yang CY, Chang TJ, Wu YH and Lee TW: Biodistribution and pharmacokinetics of transgenic pig-produced recombinant human factor IX (rhFIX) in rats. In Vivo *22*: 693-697, 2008.

24 Pelosi G, Volante M, Papotti M, Sonzogni A, Masullo M and Viale G: Peptide receptors in neuroendocrine tumors of the lung as potential tools for radionuclide diagnosis and therapy. Q J Nucl Med Mol Imaging *50*: 272-287, 2006.

25 Bodei L, Ferone D, Grana CM, Cremonesi M, Signore A, Dierckx RA and Paganelli G: Peptide receptor therapies in neuroendocrine tumors. J Endocrinol Invest *32*: 360-369, 2009.

26 Thomas R, Chen J, Roudier MM, Vessella RL, Lantry LE and Nunn AD: *In vitro* binding evaluation of ^{177}Lu-AMBA, a novel 177Lu-labeled GRP-R agonist for systemic radiotherapy in human tissues. Clin Exp Metastasis *26*: 105-119, 2009.

27 Linder KE, Metcalfe E, Arunachalam T, Chen J, Eaton SM, Feng W, Fan H, Raju N, Cagnolini A, Lantry LE, Nunn AD and Swenson RE: *In vitro* and *in vivo* metabolism of Lu-AMBA, a GRP-receptor binding compound, and the synthesis and characterization of its metabolites. Bioconjug Chem *20*: 1171-1178, 2009.

28 Minn AJ, Kang Y, Serganova I, Gupta GP, Giri DD, Doubrovin M, Ponomarev V, Gerald WL, Blasberg R and Massague J: Distinct organ-specific metastatic potential of individual breast cancer cells and primary tumors. J Clin Invest *115*: 44-55, 2005.

29 Wu JC, Inubushi M, Sundaresan G, Schelbert HR and Gambhir SS: Optical imaging of cardiac reporter gene expression in living rats. Circulation *105*: 1631-1634, 2002.

30 Rogers BE, Bigott HM, McCarthy DW, Della Manna D, Kim J, Sharp TL and Welch MJ: MicroPET imaging of a gastrin-releasing peptide receptor-positive tumor in a mouse model of human prostate cancer using a ^{64}Cu-labeled bombesin analogue. Bioconjug Chem *14*: 756-763, 2003.

31 Fanger BO, Wade AC and Cardin AD: Characterization of the murine pancreatic receptor for gastrin releasing peptide and bombesin. Regul Pept *32*: 241-251, 1991.

32 Rudin M and Weissleder R: Molecular imaging in drug discovery and development. Nat Rev Drug Discov *2*: 123-131, 2003.

33 Johnson CV, Shelton T, Smith CJ, Ma L, Perry MC, Volkert WA and Hoffman TJ: Evaluation of combined ^{177}Lu-DOTA-8-AOC-BBN (7-14)NH_2 GRP receptor-targeted radiotherapy and chemotherapy in PC-3 human prostate tumor cell xenografted SCID mice. Cancer Biother Radiopharm *21*: 155-166, 2006.

34 de Visser M, Bernard HF, Erion JL, Schmidt MA, Srinivasan A, Waser B, Reubi JC, Krenning EP and de Jong M: Novel ^{111}In-labelled bombesin analogues for molecular imaging of prostate tumours. Eur J Nucl Med Mol Imaging *34*: 1228-1238, 2007.

35 Garrison JC, Rold TL, Sieckman GL, Naz F, Sublett SV, Figueroa SD, Volkert WA and Hoffman TJ: Evaluation of the pharmacokinetic effects of various linking group using the ^{111}In-DOTA-X-BBN(7-14)NH_2 structural paradigm in a prostate cancer model. Bioconjug Chem *19*: 1803-1812, 2008.

Received June 6, 2010
Revised August 6, 2010
Accepted August 24, 2010